HHS Public Access

Author manuscript

Neurotoxicology. Author manuscript; available in PMC 2019 March 01.

Published in final edited form as:

Neurotoxicology. 2018 March ; 65: 196–206. doi:10.1016/j.neuro.2017.10.004.

Exposure to Fine and Ultrafine Particulate Matter during Gestation Alters Postnatal Oligodendrocyte Maturation, Proliferation Capacity, and Myelination

Carolyn Klocke[1], **Joshua L. Allen**[1], **Marissa Sobolewski**[1], **Jason L. Blum**[2], **Judith T. Zelikoff**[2], and **Deborah A. Cory-Slechta**[1]

[1]Department of Environmental Medicine, University of Rochester School of Medicine, Rochester, NY, USA

[2]Department of Environmental Medicine, New York University School of Medicine, Tuxedo, NY, USA

Abstract

Accumulating studies indicate that the brain is a direct target of air pollution exposure during the fetal period. We have previously demonstrated that exposure to concentrated ambient particles (CAPs) during gestation produces ventriculomegaly, periventricular hypermyelination, and enlargement of the corpus callosum (CC) during postnatal development in mice. This study aimed to further characterize the cellular basis of the observed hypermyelination and determine if this outcome, among other effects, persisted as the brain matured. Analysis of CC-1^+ mature oligodendrocytes in the CC at postnatal days (PNDs) 11–15 suggest a premature maturational shift in number and proportion of total cells in prenatally CAPs-exposed males and females, with no overall change in total CC cellularity. The overall number of $Olig2^+$ lineage cells in the CC was not affected in either sex at the same postnatal timepoint. Assessment of myelin status at early brain maturity (PNDs 57–61) revealed persistent hypermyelination in CAPs-exposed animals of both sexes. In addition, ventriculomegaly was persistent in CAPs-treated females, with possible amelioration of ventriculomegaly in CAPs-exposed males. When oligodendrocyte precursor cell (OPC) pool status was analyzed at PNDs 57–61, there were significant CAPs-induced alterations in cycling $Ki67^+/Olig2^+$ cell number and proportion of total cells in the female CC. Total CC cellularity was slightly elevated in CAPs-exposed males at PNDs 57–61. Overall, these data support a growing body of evidence that demonstrate the vulnerability of the developing brain to environmental insults such as ambient particulate matter. The sensitivity of oligodendrocytes and myelin, in particular, to such an insult warrants further investigation into the mechanistic underpinnings of OPC and myelin disruption by constituent air pollutants.

Corresponding Author: Carolyn Klocke, Department of Environmental Medicine, Box EHSC, 601 Elmwood Avenue, University of Rochester School of Medicine, Rochester, NY 14642; phone: 585-273-4590, carolyn_klocke@urmc.rochester.edu.

Keywords

air pollution; particulate matter; myelin; oligodendrocyte; oligodendrocyte progenitor cell

1: Introduction

Myelination is a complex, temporally-restricted process that is highly susceptible to perturbation by extrinsic factors. The principle myelinating cells of the central nervous system (CNS), oligodendrocytes, which are a macroglial cell type found throughout the adult CNS in both mature and progenitor forms (Rowitch and Kriegstein, 2010). Once mature, oligodendrocytes function to create concentric, multilamellar, lipid-rich myelin sheaths around neuronal axons in a segmented manner, enhancing saltatory conduction for more efficient action potential propagation (Hughes and Appel, 2016). Oligodendrocytes undergo three waves of expansion in the ventral forebrain of the fetal mouse, the first of which occurs in the pre-optic area around gestational day (GD) 12.5, the second in the lateral and medial ganglionic eminences at GD15.5, and the third wave expands ventrally into the cortex at parturition (Rowitch and Kriegstein, 2010). These waves of progenitor cell expansion are facilitated by a complex dance of balanced transcriptional regulation, such as positive regulation by sonic hedgehog (Shh) gene expression patterning (Traiffort et al., 2016), and subsequent OPC differentiation and maturation is dependent upon the inhibition of neuronal specification and self-renewal signaling (Rowitch, 2004). Thus, oligodendrocyte progenitor cells (OPCs) require a precise orchestration of both environmental and genetic cues for successful specification, differentiation, and maturation (Emery, 2010; He and Lu, 2013). Perturbations of the local microenvironment can result in aberrant gene expression patterning and disrupted OPC maturation, which, ultimately, could result in alterations in myelination (El Waly et al., 2014; Volpe et al., 2011). Further, a cycling pool of OPCs is maintained throughout the life of the organism, providing a potential mechanism by which myelin can be repaired if myelinated axons have experienced injury or damage (Armstrong et al., 2016; Kang et al., 2010).

Several lineage-specific transcription factors are implicated in the specification and differentiation of OPCs (Wang et al., 2014). Among these transcription factors is Olig2, a marker that is expressed in OPCs and signals fate specification of neural stem cells to the oligodendrocyte lineage (Zhu et al., 2012). Olig2 and the closely-related Olig1 are basic helix-loop-helix (bHLH) transcription factors that inhibit astrocytic and neuronal specification in neural stem cells (Zhou and Anderson, 2002). Olig2 is considered the primary determinant of oligodendrocyte specification (Rowitch, 2004), and studies have shown that Olig2 ablation in OPCs is sufficient to attenuate differentiation and myelination in the spinal cord (Lu et al., 2002; Takebayashi et al., 2002). In contrast, Olig2 ablation in mature oligodendrocytes results in accelerated maturation and myelination (Mei et al., 2013). Indeed, Olig2 is known to be expressed throughout the oligodendrocyte lineage (Zhou and Anderson, 2002); however, its importance in OPC fate specification makes it an ideal candidate for determining if gestational exposure to air pollution impacts OPC specification in the CC.

Adenomatous polyposis coli (APC) is a tumor suppressor protein that is expressed in the large intestine and in the CNS, although its CNS expression is limited almost exclusively to neurons and mature oligodendrocytes (Bhat et al., 1996; Fancy et al., 2014). In oligodendrocytes, APC (clone CC-1) appears at maturation and the onset of myelination (Lang et al., 2013) and is thought to regulate glial process extension via canonical wingless and integration site (Wnt)/β-catenin signaling pathways (Dai et al., 2014). Though the mechanisms of APC (CC-1)-mediated OPC maturation and myelination are not well understood, this protein is potentially crucial for successful CNS myelination. APC itself is a widely-expressed tumor suppressor protein in the CNS. However, it has been verified that the expression of clone CC-1 is restricted to oligodendrocytes, whereas original APC is found in neurons (Brakeman et al., 1999). Allelic deficiency of APC (CC-1) was shown to negatively impact the onset of myelination as a consequence of attenuated oligodendrocyte maturation (Fancy et al., 2009; Lang et al., 2013). These studies highlight the importance of this protein in oligodendrocyte maturation and its potential role as a target of gestational air pollution exposure.

Myelination is of critical mechanistic importance. Several lines of epidemiological evidence have shown that environmental insult during developmental periods increases risk and/or susceptibility to aberrant white matter tract formation and myelinating disorders later in life. Air pollution-derived particulate matter (PM) exposure during fetal development periods have been implicated in the etiology of neurodevelopmental disorders such as autism spectrum disorder (ASD), among others (Talbott et al., 2015; Volk et al., 2013). Psychosocial disorders such as ASD often present with white matter abnormalities, such as either enlargement or reduction in the volume of the CC, the largest white matter tract in the brain, critical to hemispheric connectivity (Hardan et al., 2009; Lefebvre et al., 2015; Travers et al., 2015; Wolff et al., 2012). Additionally, air pollution exposure has been linked to the development of multiple sclerosis (MS), a demyelinating disease with no current cure (Calderon-Garciduenas et al., 2016; Esmaeil Mousavi et al., 2017; Heydarpour et al., 2014; Vojinovic et al., 2015). This growing body of evidence highlights the need to further understand the mechanistic underpinnings of air pollution neurotoxicity, with specific regard to developmental white matter dysregulation, as white matter alterations could potentially persist into adulthood and permanently affect neurocognitive processes.

This study sought to test whether gestational exposure to CAPs can alter maturation of the oligodendrocyte lineage and increase oligodendrocyte numbers in the CC. These findings could provide a mechanistic basis for the previously observed hypermyelination in this region. Further, we sought to determine if the hypermyelination previously observed during (PNDs 11–15; Klocke et al., 2017), following gestational exposures, persisted into early maturity, which would indicate that fetal neurodevelopmental processes are susceptible to long-term alteration by particulate matter.

2: Methods

2.1: Animals and Air Pollution Exposures

PM exposures were carried out as previously described (Blum et al., 2017; Klocke et al., 2017). Briefly, male and female (8–10 week-old) B6C3F$_1$ hybrid mice were bred

monogamously. Upon discovery of a coital plug, GD0.5, females were placed into the exposure chamber. Pregnant dams (N = 16) were then exposed to concentrated ambient particles (CAPs) or HEPA-filtered air (FA) via compartmentalized whole-body inhalation for 6 hrs/day from GD0.5 through GD16.5 using the Versatile Aerosol Concentration Enrichment System (VACES). The VACES, fully characterized in Maciejczyk et al. (2005), selectively concentrates fine (≤ 2.5 μm diameter) and ultrafine (≤ 100 nm diameter) ambient PM from a local highway near the New York University Department of Environmental Medicine in Sterling Forest, NY. Exposures occurred between 0800–1400 hours during August of 2014. Dams had access to food and water *ad libitum* except during exposures and no overt toxicity was observed among the exposed animals. Mass concentration and elemental composition of these CAPs exposures were previously determined and reported (Klocke et al., 2017).

Upon conclusion of exposures at GD16.5, dams were maintained in ambient air through birth and the postnatal period. No offspring mortality was observed. Final sample numbers considered at the early postnatal timepoint (PND11–15) were: 11 female FA, 7 female CAPs, 9 male FA, and 6 male CAPs from 5–6 litters/treatment group (total N = 33 offspring). Final sample numbers for the late timepoint (PND57–61) were: 8 female FA, 7 female CAPs, 9 male FA, and 8 male CAPs (total N = 32 offspring). Sex of the offspring was determined by visual examination at PND11. Mice used in this study were treated humanely and all study protocols were approved by the New York University Institutional Animal Care and Use Committee.

2.2: Immunohistochemistry and Fluorescent Immunostaining

Pups were sacrificed by rapid decapitation between PNDs 11–15 and 57–61 and brain tissue was processed for immunostaining as previously described (Klocke et al., 2017). For quantification of immature and mature oligodendrocytes in the postnatal CC at PNDs 11–15, tissue was incubated with primary antibodies against Olig2 (1:200; EMD Millipore, Billerica, MA) and adenomatous polyposis coli (APC), clone CC-1 (CC-1, 1:200; EMD Millipore), respectively. To assess persistent effects of CAPs on the CC at PNDs 57–61, myelination and markers of proliferation (Ki67; 1:200; Sigma-Aldrich, St. Louis, MO) and glial lineage (Olig2) were analyzed. Myelination status of the CC was determined utilizing immunohistochemistry and immunofluorescence with antibodies against myelin basic protein (MBP; 1:1000; Millipore, Billerica, MA), and with the fluorescent stain FluoroMyelin Red performed according to manufacturer's instructions (ThermoFisher Scientific, Waltham, MA). To determine the effect of CAPs on the oligodendrocyte precursor pool and lineage, tissue was incubated with antibodies against Ki67 (1:250; ThermoFisher Scientific) and Olig2 (1:200; EMD Millipore). For both timepoints, secondary antibodies conjugated to fluorophores Alexa Fluor 488 and 594 were used for fluorescent detection (1:1000; Abcam) and DAPI (4',6-diamidino-2-phenylindole) was used as a global nuclear stain (1:5000; ThermoFisher Scientific).

2.3: Stereological Quantification of Oligodendrocytes and Glial Progenitors

All stereological analyses were performed in a blinded manner. Slides were visualized on an Olympus BX41 microscope (Olympus America, Inc., Central Valley, PA) mounted with an

MBF CX9000 camera (MBF Bioscience, Villiston, VT) for detection of immunofluorescence. Stereo Investigator (MBF Bioscience) was used to enumerate the total number of immature and mature oligodendrocytes. The optical fractionator probe was used to sample at least 15% of three major CC sub-regions (splenium, midbody, and genu) across 3 serial tissue sections for quantitative assessment of Olig2/CC-1 at PNDs 11–15. The same probe was used to sample at least 10% of the entire CC across 3 serial tissue sections for quantitative assessment of Ki67/Olig2 at PNDs 57–61. The mean thickness of each section was determined in 3 fields across all 3 tissue sections, and the upper and lower 0.5μm limits were excluded from analysis. For assessment of Olig2/CC-1 at PNDs 11–15, cells positive for Olig2 and CC-1 immunofluorescence were marked and any co-localization of the two markers in the same cell ($Olig2^+/CC\text{-}1^+$) was confirmed by cross-referencing the DAPI channel. The remaining $Olig2^-/CC\text{-}1^-/DAPI^+$ cells were enumerated to provide an estimate of the total cellularity of each CC sub-region. $Olig2^+$, $CC\text{-}1^+$, $Olig2^+/CC\text{-}1^+$ double stained cells, and $DAPI^+$ cells are reported as total estimates as quantified by the software. The same approach for determining co-localization was utilized for tissue stained for Ki67/Olig2 at PNDs 57–61.

2.4: Determination of Ventricular Area and Myelin Density

All densitometric analyses were performed in a blinded manner. Lateral ventricle and CC area tracings were sampled across three tissue sections for each region of interest as previously described (Klocke et al., 2017). Due to the spatial variability in ventricular size throughout the brain, areas from three tissue sections throughout the brain were measured to illustrate any discrete changes in regional ventricular area. Thus, ventricular area is presented linearly (lateral-most section to medial-most section) with each data point equal to a single tissue section. A murine anatomical brain atlas (Franklin and Paxinos, 2007) was utilized in conjunction with identification of anatomical landmarks to ensure that sections of homologous bregma were analyzed. The approximate area analyzed in tissue sections per endpoint ranged from 0.12–1.68 mm lateral to the midline bregma, with slight variation due to brain size variability between sexes and treatment groups which may have affected tissue sectioning. To quantify myelin staining density, montage images were captured at 20× in the brightfield (MBP) or Texas Red fluorescent channel (FluoroMyelin) using Neurolucida software (MBF, Williston, VT). Subdivision of the CC was performed as previously described by Tanaka-Arakawa et al. (2015) with slight modifications. Identified CC subregions were analyzed using established thresholding methods (Cherry et al., 2014) in ImageJ (National Institutes of Health, Bethesda, MD) to generate the percent of positive staining relative to CC area.

2.5: Statistical Analyses

Statistical analyses were conducted using JMP Pro 12.0 (SAS Institute Inc., Cary, NC). Lateral ventricle and CC area measurements were analyzed separately by sex using a repeated measures ANOVA with treatment group (CAPs or FA) and PND as fully factorial, between-group factors and tissue section as a continuous, within-group factor. Lateral ventricle area analysis was weighted by PND based on previous observations in which PND significantly affected the analysis of this endpoint (Klocke et al., 2017). Numbers of immature and mature oligodendrocytes, as well as remaining cells, were analyzed separately

by sex using one-way ANOVAs. *Post hoc* testing was conducted contingent on ANOVA outcomes using Student's t-test. Statistically significant outliers were determined via Grubbs test and were excluded from analyses. P values ≤ 0.05 were considered statistically significant.

3: Results

3.1: CAPs Exposure Data

As previously reported in Klocke et al. (2017), the mass concentration of CAPs exposures throughout the course of gestation averaged 92.7 ± 19.2 μg/m^3 (mean ± SD) for CAPs exposure chambers and 3.5 ± 0.9 μg/m^3 for FA control chambers. There was temporal (i.e. day-to-day) variability in the CAPs exposures, with average daily levels ranging from 33.0 μg/m^3 to 184.4 μg/m^3.

3.2: Postnatal Oligodendrocyte Maturation

Stereological quantification of Olig2$^+$ and CC-1$^+$ cells was conducted in the splenium, midbody, and genu sub-regions of the CC to determine the effect of gestational exposure to CAPs on postnatal oligodendrocyte maturation. At PNDs 11–15, gestational CAPs exposure significantly affected the number (Figure 1) and percentage (Figure 2) of mature, CC-1$^+$ oligodendrocytes in each sub-region for both sexes. In the caudal splenium sub-region of the CC, CAPs significantly increased the number of CC-1$^+$ cells in females [$F(1,16) = 5.33$, $p = 0.035$; Figure 1a] and males [$F(1,13) = 6.023$, $p = 0.029$; Figure 1a]. CAPs also significantly increased CC-1$^+$ number in the midbody sub-region of females [$F(1,15) = 11.10$, $p = 0.0046$; Figure 1b] and males [$F(1,12) = 16.33$, $p = 0.0016$; Figure 1b]. The genu sub-region experienced an increase in CC-1$^+$ cells in CAPs-treated females [$F(1,14) = 51.80$, $p < 0.0001$; Figure 1c] and males [$F(1,13) = 26.081$, $p = 0.0002$; Figure 1c]. In the female genu, significant increase in Olig2$^-$/CC-1$^-$/DAPI$^+$ nuclei were observed [$F(1,14) = 9.70$, $p = 0.0076$; Figure 1c], suggesting increased cellularity of other cell types in this sub-region, which could include astrocytes, microglia, and vascular endothelial cells. Analysis of cell number in all three combined sub-regions revealed an overall total CC increase in CC-1$^+$ staining in females [$F(1,16) = 26.70$, $p < 0.0001$; Figure 1d] and males [$F(1,13) = 20.44$, $p = 0.0006$; Figure 1d]. In the female CC, there was a tendency towards increased DAPI$^+$ nuclei due to CAPs treatment [$F(1,16) = 3.075$, $p = 0.099$; Figure 1d]. There was also a suggestion of a decrease in Olig2$^+$ cells in the male CC, although it did not reach statistical significance [$p = 0.10$; Figure 1d]. Overall, CAPs appears to increase the number of CC-1$^+$ cells in juvenile male and female offspring globally in the CC and within its sub-regions.

Cell counts are expressed as a percent of total cells to determine if changes in number for each marker are indicative of a proportional change with respect to the total number of cells within the CC. The numbers of Olig2$^+$, CC-1$^+$, and DAPI$^+$ cells trended similarly when expressed as a proportion of total cells, with the proportion of CC-1$^+$ cells significantly elevated in each CC sub-region and in the CC as a whole (Figure 2a–c). In the splenium, the proportion of CC-1$^+$ cells was elevated significantly in CAPs-treated females at PNDs 11–15 [$F(1,16) = 5.15$, $p = 0.037$; Figure 2a] and same-aged males [$F(1,13) = 10.51$, $p = 0.0064$; Figure 2a]. In the midbody region, the effect of CAPs on numbers of CC-1$^+$ cells was

significant in females [F(1,15) = 11.10, $p = 0.0046$; Figure 2b] and males [F(1,12) = 41.77, $p < 0.0001$; Figure 2b]. CAPs also decreased the proportion of $Olig2^+$ cells in the male midbody, but the effect was not significant [$p = 0.10$; Figure 2b]. There was no significant effect of CAPs on the proportion of $DAPI^+$ cells in any CC sub-region or across the CC as a whole (Figure 2d).

Olig2 is an oligodendrocyte pan-lineage marker (Harrington et al., 2010), and it would be expected that $CC\text{-}1^+$ cells would retain expression and immunoreactivity against Olig2. Therefore, co-localization of Olig2 and CC-1 was determined in each sub-region of the CC to determine the fraction of oligodendrocytes that express both markers. There was a trending elevation in mature $Olig2^+/CC\text{-}1^+$ oligodendrocytes in the male genu [F(1,13) = 2.84, $p = 0.12$; Figure 3c], but no significant change in the female genu, nor the splenium or midbody of either sex. Interestingly, the number of $Olig2^+/CC\text{-}1^+$ oligodendrocytes was an order of magnitude lower than $Olig2^+/CC\text{-}1^-$ cells or $Olig2^-/CC\text{-}1^+$cells, suggesting loss of oligodendrocyte Olig2 expression at maturation [Figure 1 vs. Figure 3].

Analysis of total cell number estimates revealed no change in total cellularity due to CAPs exposure in the splenium or midbody sub-regions of either sex (Figure 4a). CAPs exposure caused a minimal elevation ($p = 0.055$), in the number of cells in the female genu which coincides with the trending increase in $Olig2^+/CC\text{-}1^+$ cells observed in this sub-region (Figure 3a). In contrast, gestational CAPs exposure had no significant effect on cell number in the male genu ($p = 0.097$; Figure 4a). When stereological estimates from all sub-regions were analyzed together, cell number across the CC as a whole were not significantly affected by gestational exposure to CAPs in either sex (Figure 4b).

3.3: Persistent Periventricular White Matter Pathology

Lateral ventricle area tracings were analyzed followed by analysis of myelin density. Surprisingly, ventricular area was found to be persistently elevated in females at PNDs 57–61 with trending significance when analyzed by repeated measures ANOVA and weighted by PND [F(1,14) = 3.58, $p = 0.08$; Figure 5a]. Interestingly, the persistence of this effect was sex-specific and not observed in males. Corpus collosum area remained persistently enlarged in CAPs-exposed males, but not females, when analyzed separately and unweighted by PND, by multivariate analyses [F(1,13) = 5.18, $p = 0.040$; Figure 5b]. There was an overall effect of CAPs when sex was added as a within-group factor in the model [F(1, 25) = 7.25, $p = 0.013$], and an interaction of CAPs and PND [F(1,25) = 6.34, $p = 0.019$].

Staining intensity of myelin basic protein (MBP) and FluoroMyelin Red were determined at PNDs 57–61, a period of more advanced CNS maturity, to determine if the periventricular hypermyelination observed at PNDs 11–15 was persistent. Consistent with the observations at PND 11–15, MBP staining intensity was significantly elevated in the CC across the splenium, midbody, and genu at PNDs 57–61 when analyzed by multivariate analyses [main effect of CAPs, F(1,25) = 33.75, $p < 0.0001$; Figure 6]. Similarly, FluoroMyelin Red staining intensity was found to be significantly elevated in CAPs-treated offspring at PNDs 57–61 [main effect of CAPs, F(1,26) = 22.66, $p < 0.0001$; Figure 7]. There was a significant effect of PND at this same timepoint for the FluoroMyelin analysis [F(1,26) = 11.49, $p = 0.0022$].

3.4: Cycling Glial Progenitor Cells in the Mature CC

Late timepoint (PNDs 57–61) tissue was stained for Ki67, a marker of proliferation, and Olig2, a marker of immature glial lineage cells and stereological quantification of these markers was performed for the entire CC. In CAPs-exposed females, the estimated number of singly-stained $Ki67^+$ cells in the CC was significantly elevated compared to controls [$F(1,7) = 14.086$, $p = 0.0095$; Figure 8a]. Alternatively, there was no effect of CAPs on $Olig2^+$ or $DAPI^+$ cells in the female CC. In males, gestational CAPs exposure significantly elevated the number of singly-stained $DAPI^+$ cells in the CC [$F(1,8) = 6.24$, $p = 0.041$; Figure 8a], indicative of increased cellularity of cell types that were not characterized by this analysis (e.g. microglia, astrocytes, etc.).

In considering immature glial progenitors, gestational CAPs exposure significantly elevated the estimated number of double-positive $Ki67^+/Olig2^+$ cells in the female CC [$F(1,7) = 12.84$, $p = 0.012$; Figure 8b]. There was no effect of CAPs exposure on the number of $Ki67^+/Olig2^+$ cells in the male CC. There was a marginally significant sex effect within the CAPs-exposed group in which females had significantly elevated levels of double-positive $Ki67^+/Olig2^+$ cells compared to males [$F(1,7) = 5.93$, $p = 0.051$; Figure 8b]. Gestational CAPs exposure did not significantly affect the total estimated number of cells in the CC in females, but there was a trending elevation in CAPs-exposed males [$F(1,8) = 3.74$, $p = 0.095$; Figure 8c].

The proportion of positively-stained $Ki67^+$ and $Olig2^+$ cells relative to the total number of cells was quantified. Gestational CAPs exposure did not significantly affect the proportion of singly-stained $Ki67^+$ cells in the CC, though there was a trending elevation [$F(1,7) = 4.41$, $p = 0.08$; Figure 9a]. There was no effect of CAPs on the proportion of $Ki67^+$, $Olig2^+$, or $DAPI^+$ cells in the male CC. In contrast, there was a significant elevation of double-positive $Ki67^+/Olig2^+$ cells in the female CC [$F(1,7) = 8.10$, $p = 0.029$; Figure 9b] and a trending effect of sex between CAPs-exposed females and males [$F(1,7) = 5.93$, $p = 0.051$; Figure 9c].

4: Discussion

We previously reported that gestational exposure to air pollution-derived PM in concentrated form is capable of inducing excess myelination, i.e. hypermyelination or white matter overgrowth, in the CC at PNDs 11–15 (Klocke et al., 2017). The concentration of CAPs utilized in this study is comparable to ambient PM concentrations experienced in Beijing, China (Sun et al., 2004) Another previous study in mice demonstrated that PNDs 4–7 and 10–13 are also sensitive windows for PM exposure in regards to myelin (Allen et al., 2014). In contrast to the hypermyelination observed following gestational PM exposure, hypomyelination was seen when PM exposure occurred during the postnatal period. Differences in myelin phenotype observed via maternal/gestational exposure compared to postnatal-only exposure underscore the importance of exposure timing in the context of white matter abnormalities. The gestational PM exposures performed in this study encompassed a period of stem cell migration, differentiation, and maturation in contrast to previous postnatal exposures, which took place during a period of peak oligodendrocyte differentiation and compact myelin formation (Vincze et al., 2008). The fact that an

exposure during either period shares a physiological target and results in white matter damage suggests that PM directly targets developing myelin, potentially by targeting of oligodendrocytes, the myelin-forming cells of the brain.

Here, we present evidence that exposure to CAPs during gestation accelerates CC oligodendrocyte maturation in the absence of changes in total oligodendrocyte number during the postnatal period, an effect that is likely contributing to persistently elevated myelin levels in each subregion of the CC. Additionally, gestational CAPs exposure appears to significantly affect the proliferative capacity of cells in the female CC at maturity (PNDs 57–61), which includes glial progenitor cells. Accelerated oligodendrocyte maturation at PNDs 11–15 provides a basis for the previous observation of hypermyelination at this timepoint (Klocke et al., 2017). However, the persistence of hypermyelination at PNDs 57–61 raises questions as to the potential mechanisms driving myelin repair given that the structural integrity of myelin sheaths was found to be compromised at PNDs 11–15 (Klocke et al., in preparation). It is possible that early damage to the myelin sheaths at PNDs 11–15 initiated repair mechanisms in oligodendrocytes that resulted in additional myelin formation. This hypothesis is supported by the observation of elevated numbers of glial progenitors at PNDs 57–61. However, this study did not directly test whether myelin repair contributed to persistent hypermyelination, therefore future studies should be performed to elucidate any contribution these mechanisms.

Initially, we hypothesized that CAPs exposure would result in an increase in CC-1^+ cells, a phenotype which would be consistent with an accelerated OPC maturation. However, in each major CC subregion, there was little to no significant effect of CAPs on the number or proportion of $Olig2^+$ cells, indicating that the OPC pool was not affected by CAPs at PNDs 11–15. In addition, quantification of these markers in the major CC subregions did not show discrete regional differences in OPC maturation between treatment groups in either sex, with the singular exception being the genu in which there was a significant decrease in $Olig2^+$ cells in both male and female offspring at PNDs 11–15. The genu is the most rostral portion of the CC and contributes to interhemispheric connectivity of the frontal and premotor cortices (Mack et al., 1995); functionally, the loss of $Olig2^+$ cells and concurrent accelerated oligodendrocyte maturation in this region result in alterations in executive and motor functions (Mathew et al., 2013; Schulte and Muller-Oehring, 2010). Such neurobehavioral deficits are characteristic of disorders associated with gestational air pollution exposure in epidemiological studies, such as ASD (Hoffmann et al., 2016; McPhillips et al., 2014). However, these deficits are typically concurrent with altered interhemispheric connectivity, i.e. alterations in neuronal signaling between cerebral hemispheres (Blatt, 2012).

Given that the functional consequences of elevated numbers of oligodendrocytes and hypermyelination as a result of CAPs exposure are not yet known, it is difficult to speculate the potential for neurobehavioral alterations due to this phenotype and whether it would correlate with those observed in neurodevelopmental disorders. However, we can predict that interhemispheric signaling would indeed be perturbed, as any deviation from the optimal amount of myelin on a given axon is likely to perturb neuronal signaling (Adlkofer et al., 1995). Analyses that could test for functional myelin deficits include behavioral tests such as locomotor activity and rotarod assays (Deacon, 2013) as well as *ex vivo* electrophysiological

assessments, such as experimentally-induced compound action potentials to quantitatively assess the action potential latency of myelinated axons (Diouf et al., 2016).

Indeed, the phenotype of persistent hypermyelination is particularly intriguing due to observations of increased myelin sheath thickness in the postnatal period and concomitant sites of focal damage in the midbody subregion of the CC (Klocke et al., in preparation). Typically, myelin sheath damage would result in activation of microglia and the release of proinflammatory mediators (Chew et al., 2013), which would hypothetically result in additional damage to the myelin sheath (Kroner et al., 2014). The observation of iron (Fe) deposition in these regions (Klocke et al., 2017) suggests that a more complex interplay is occurring between oligodendrocyte maturation, myelin damage, and microglial activation. Elemental Fe in the ferric (Fe^{3+}) state is a driver of oligodendrocyte maturation and myelin biosynthesis (Badaracco et al., 2010; Connor and Menzies, 1996). It is possible that Fe may be driving accelerated OPC maturation and myelin formation in the CC, while also inducing microglial activation, as microglia would be the primary phagocytic clearance mechanism of inorganic particles in the CNS (Wang et al., 2011). The kinetics of Fe deposition and clearance in the fetal CNS as a result of CAPs exposures are not known. Thus, it is unclear at which point during gestation deposition of Fe in the fetal brain might have occurred. If Fe was able to reach a fetus early in gestation, prior to the initial wave of oligodendrocyte expansion at GD12.5 (Rowitch and Kriegstein, 2010), it is possible that the presence of Fe in the fetal CNS could accelerate OPC maturation, resulting in the shift towards a CC-1^{+} maturation phenotype and thus result in hypermyelination. However, the persistence of excess myelin to early maturity (PNDs 57–61) is somewhat contradictory considering the focal damage to the myelin sheaths (Klocke et al., submitted manuscript) and concurrent microglial activation observed at PNDs 11–15 (Klocke et al., 2017). It is possible excess Fe both drives OPC maturation and excess myelin production in addition to damaging said myelin. This damage could be driven by both activated microglia as well as excess Fe, which can result in the production of reactive oxygen species (ROS) via the Fenton reaction (Mehlhase et al., 2006). The persistent hypermyelination observed in CAPs-exposed mice may be reflective of myelin repair processes initiated in response to focal myelin sheath damage or as a result of altered Fe metabolism. Myelin biosynthesis is an energy-intensive process that requires elemental Fe (Connor and Menzies, 1996), and it is possible that elevated levels of Fe in the developing CNS as a result of CAPs exposure may alter baseline Fe metabolism and thus result in altered myelination. Overall, it appears that the effects of excess Fe in the developing brain are complex and will require further investigation.

The persistence of CC hypermyelination at PNDs 57–61 suggests the existence of a compensatory mechanism that could lead to amelioration of the damaged myelin in a persistent manner. Indeed, myelin has the capacity to regenerate itself after injury to the axon or myelin sheath itself (Armstrong et al., 2016). However, regenerated myelin is typically thinner with altered internodal distances (Brill et al., 1977). It is unclear whether gestational CAPs exposure contributes to alterations in myelin internodal distance. However, the increased MBP and FluoroMyelin staining densities observed here suggest that excess myelin is present and thinning of the sheath does not occur. Evidence suggesting that repair mechanisms may be activated is indicated by persistent elevation in numbers of Ki67^{+}/Olig2^{+} glial progenitors in the CC at PNDs 57–61. This observed effect was shown in this

study to be female-specific, which corresponds to the effect of persistent ventriculomegaly in females, and suggests that myelin repair mechanisms may be sexually dimorphic. A limitation of this hypothesis is that $Ki67^{+}/Olig2^{+}$ will stain both proliferative OPCs and proliferative astrocytic progenitors.

The process of oligodendrogenesis is inhibitory to the formation of astrocytes, and astrocytes eventually stop expressing Olig2 as they mature (Rowitch, 2004). Despite that quantification of $Ki67^{+}/Olig2^{+}$ progenitors is indicative of both OPCs and astrocyte progenitors, it is still possible that the elevated level of cycling glial progenitors could contribute to the phenotype of persistent CC hypermyelination. Taken together, further investigation is required to elucidate the ultrastructural pathology and functional consequences of persistent hypermyelination.

In considering potential oligodendroglial signaling mechanisms, studies investigating OPC maturation and myelin pathways in neurodevelopment have demonstrated the importance of extracellular regulated kinase/mitogen-activated protein kinase (ERK/MAPK) signaling in oligodendrocytes as a promoter of OPC expansion and an important determinant of myelin sheath thickness (Ishii et al., 2012). Transgenic mice with constitutively active ERK1/2 in 2’3’-cyclic nucleotide 3’-phosphodiesterase^{+} (CNP^{+}) OPCs appear to have persistent hypermyelination throughout adulthood in the form of increased myelin sheath thickness oligodendrocyte cell body size (Fyffe-Maricich et al., 2013). The same investigators also demonstrated deletion of ERK1/2 in OPCs in mice resulting in impaired ability to myelinate axons (Ishii et al., 2012) and that loss of ERK2 alone was sufficient to delay MBP expression in the CC at PND10 (Fyffe-Maricich et al., 2011). The CC-1 clone of APC is a positive regulator of oligodendroglial maturation (Lang et al., 2013). Signaling pathway crosstalk of APC (CC-1) occurs with the ERK/MAPK pathway via canonical Wnt/β-catenin signaling (Chew et al., 2010). As APC (CC-1) a negative regulator of β-catenin, it is possible that upregulation of APC (CC-1) and/or lack of β-catenin activation, in conjunction with ERK/MAPK pathway upregulation, could underlie accelerated OPC maturation and persistent hypermyelination observed in this study (Gaesser and Fyffe-Maricich, 2016). Extensive studies are required to elucidate the contributions, if any, of these signaling pathways to CAPs-induced hypermyelination. However, the observed increase in $CC\text{-}1^{+}$ oligodendrocytes in the CC region strongly suggests at least some involvement of these pathways.

It would be highly informative to perform additional gestational CAPs exposures with the goal of elucidating the developmental timing behind accelerated OPC maturation in the CC as an underpinning of hypermyelination using knockout mouse models. One possibility would consist of a time-course study in which conditional ablation of APC is performed at different gestational and postnatal timepoints to elucidate the temporal relationships of CAPs-induced hypermyelination and determine at which developmental stage CAPs exposure drives OPC maturation (Lang et al., 2013). Ablation performed at critical periods of OPC development and maturation (i.e. GDs 12.5–15.5 and PNDs 10–14; Rowitch and Kriegstein, 2010), in conjunction with CAPs exposures, would allow the characterization of the temporal relationship between accelerated OPC maturation and CAPs exposure. Additionally, future studies could utilize mouse models of APC overexpression with and

without the administration of Fe to determine if accelerated oligodendrocyte maturation is sufficient to drive hypermyelination and if the presence of Fe exacerbates this effect. It would also be useful to determine the timing of such an effect and whether it occurs during one of the waves of gestational OPC expansion (Rowitch and Kriegstein, 2010) or prior to the onset of myelination (prior to PND10) using a time-course exposure design. Understanding the mechanistic basis of an accelerated OPC maturation phenotype has implications for understanding the etiology of neurodevelopmental disorders characterized by white matter overgrowth, such as ASD.

5: Conclusions

This study presents evidence demonstrating the specific vulnerability of OPCs and myelin to gestational PM exposure and highlights the potential of PM to persistently alter the trajectory of OPC maturation and myelination, observations which extend our understanding of potential mechanisms by which air pollution exposure may contribute to white matter abnormalities. Such effects are a public health concern, as any disruption of neurodevelopment could lead to functional deficits in children and adults, although further analyses are needed to determine the specific consequences of hypermyelination in a cognitive and behavioral context.

Acknowledgments

Acknowledgements and Funding Information

This work was supported by the National Institutes of Environmental Health Sciences [grant numbers P30 ES001247 and R01 ES025541 to D.A.C.-S.; T32 ES07026 (B. P. Lawrence), and P30 ES000260; M. Costa, PI], and March of Dimes (21-F12-13) to J.T.Z. Author J.L. Allen assisted in this study while at the University of Rochester but now works for Battelle Memorial Institute.

References

Adlkofer K, et al. Hypermyelination and demyelinating peripheral neuropathy in Pmp22-deficient mice. Nat. Genet. 1995; 11(3):274–280. [PubMed: 7581450]

Allen JL, et al. Early postnatal exposure to ultrafine particulate matter air pollution: persistent ventriculomegaly, neurochemical disruption, and glial activation preferentially in male mice. Environ. Health Perspect. 2014; 122(9):939–945. [PubMed: 24901756]

Armstrong RC, et al. Myelin and oligodendrocyte lineage cells in white matter pathology and plasticity after traumatic brain injury. Neuropharmacology. 2016; 110(Pt B):654–659. [PubMed: 25963414]

Badaracco ME, et al. Oligodendrogenesis: the role of iron. Biofactors. 2010; 36(2):98–102. [PubMed: 20336710]

Bhat RV, et al. Expression of the APC tumor suppressor protein in oligodendroglia. Glia. 1996; 17(2): 169–174. [PubMed: 8776583]

Blatt GJ. The neuropathology of autism. Scientifica (Cairo). 2012; 2012:703675. [PubMed: 24278731]

Blum JL, et al. Exposure to Ambient Particulate Matter during Specific Gestational Periods Produces Adverse Obstetric Consequences in Mice. Environ. Health Perspect. 2017

Brakeman JS, et al. Neuronal localization of the Adenomatous polyposis coli tumor suppressor protein. Neuroscience. 1999; 91(2):661–672. [PubMed: 10366023]

Brill MH, et al. Conduction velocity and spike configuration in myelinated fibres: computed dependence on internode distance. J. Neurol. Neurosurg. Psychiatry. 1977; 40(8):769–774. [PubMed: 925697]

Calderon-Garciduenas L, et al. Air pollution, a rising environmental risk factor for cognition, neuroinflammation and neurodegeneration: The clinical impact on children and beyond. Rev. Neurol. (Paris). 2016; 172(1):69–80. [PubMed: 26718591]

Cherry JD, et al. Neuroinflammation and M2 microglia: the good, the bad, and the inflamed. J. Neuroinflammation. 2014; 11:98. [PubMed: 24889886]

Chew LJ, et al. Mechanisms of regulation of oligodendrocyte development by p38 mitogen-activated protein kinase. J. Neurosci. 2010; 30(33):11011–11027. [PubMed: 20720108]

Chew LJ, et al. Oligodendroglial alterations and the role of microglia in white matter injury: relevance to schizophrenia. Dev. Neurosci. 2013; 35(2–3):102–129. [PubMed: 23446060]

Connor JR, Menzies SL. Relationship of iron to oligodendrocytes and myelination. Glia. 1996; 17(2): 83–93. [PubMed: 8776576]

Dai ZM, et al. Stage-specific regulation of oligodendrocyte development by Wnt/beta-catenin signaling. J. Neurosci. 2014; 34(25):8467–8473. [PubMed: 24948802]

Deacon RM. Measuring motor coordination in mice. Journal of Visualized Experiments : JoVE. 2013; (75):e2609. [PubMed: 23748408]

Diouf B, et al. Msh2 deficiency leads to dysmyelination of the corpus callosum, impaired locomotion, and altered sensory function in mice. Sci. Rep. 2016; 6:30757. [PubMed: 27476972]

El Waly B, et al. Oligodendrogenesis in the normal and pathological central nervous system. Front. Neurosci. 2014; 8:145. [PubMed: 24971048]

Emery B. Regulation of oligodendrocyte differentiation and myelination. Science. 2010; 330(6005): 779–782. [PubMed: 21051629]

Esmaeil Mousavi S, et al. Multiple sclerosis and air pollution exposure: Mechanisms toward brain autoimmunity. Med. Hypotheses. 2017; 100:23–30. [PubMed: 28236843]

Fancy SP, et al. Dysregulation of the Wnt pathway inhibits timely myelination and remyelination in the mammalian CNS. Genes Dev. 2009; 23(13):1571–1585. [PubMed: 19515974]

Fancy SP, et al. Parallel states of pathological Wnt signaling in neonatal brain injury and colon cancer. Nat. Neurosci. 2014; 17(4):506–512. [PubMed: 24609463]

Franklin, KBJ., Paxinos, G. The Mouse Brain in Stereotaxic Coordinates. Third. Elsevier, Inc; New York: 2007.

Fyffe-Maricich SL, et al. The ERK2 mitogen-activated protein kinase regulates the timing of oligodendrocyte differentiation. J. Neurosci. 2011; 31(3):843–850. [PubMed: 21248107]

Fyffe-Maricich SL, et al. Signaling through ERK1/2 controls myelin thickness during myelin repair in the adult central nervous system. J. Neurosci. 2013; 33(47):18402–18408. [PubMed: 24259565]

Gaesser JM, Fyffe-Maricich SL. Intracellular signaling pathway regulation of myelination and remyelination in the CNS. Exp. Neurol. 2016; 283(Pt B):501–511. [PubMed: 26957369]

Hardan AY, et al. Corpus callosum volume in children with autism. Psychiatry Res. 2009; 174(1):57–61. [PubMed: 19781917]

Harrington EP, et al. Oligodendrocyte PTEN is required for myelin and axonal integrity, not remyelination. Ann. Neurol. 2010; 68(5):703–716. [PubMed: 20853437]

He L, Lu QR. Coordinated control of oligodendrocyte development by extrinsic and intrinsic signaling cues. Neurosci. Bull. 2013; 29(2):129–143. [PubMed: 23494530]

Heydarpour P, et al. Potential impact of air pollution on multiple sclerosis in Tehran, Iran. Neuroepidemiology. 2014; 43(3–4):233–238. [PubMed: 25501708]

Hoffmann E, et al. Reduced functional connectivity to the frontal cortex during processing of social cues in autism spectrum disorder. Journal of neural transmission (Vienna, Austria: 1996). 2016; 123(8):937–947.

Hughes EG, Appel B. The cell biology of CNS myelination. Curr. Opin. Neurobiol. 2016; 39:93–100. [PubMed: 27152449]

Ishii A, et al. ERK1/ERK2 MAPK signaling is required to increase myelin thickness independent of oligodendrocyte differentiation and initiation of myelination. J. Neurosci. 2012; 32(26):8855–8864. [PubMed: 22745486]

Kang SH, et al. NG2+ CNS glial progenitors remain committed to the oligodendrocyte lineage in postnatal life and following neurodegeneration. Neuron. 2010; 68(4):668–681. [PubMed: 21092857]

Klocke C, et al. Neuropathological Consequences of Gestational Exposure to Concentrated Ambient Fine and Ultrafine Particles in the Mouse. Toxicol. Sci. 2017; 156(2):492–508. [PubMed: 28087836]

Klocke C, et al. Disruption of myelin sheath ultrastructure and concomitant particle inclusion formation resulting from gestational exposure to ambient particulate matter. Toxicol. Sci. submitted manuscript.

Kroner A, et al. TNF and increased intracellular iron alter macrophage polarization to a detrimental M1 phenotype in the injured spinal cord. Neuron. 2014; 83(5):1098–1116. [PubMed: 25132469]

Lang J, et al. Adenomatous polyposis coli regulates oligodendroglial development. J. Neurosci. 2013; 33(7):3113–3130. [PubMed: 23407966]

Lefebvre A, et al. Neuroanatomical Diversity of Corpus Callosum and Brain Volume in Autism: Meta-analysis, Analysis of the Autism Brain Imaging Data Exchange Project, and Simulation. Biol. Psychiatry. 2015; 78(2):126–134. [PubMed: 25850620]

Lu QR, et al. Common developmental requirement for Olig function indicates a motor neuron/oligodendrocyte connection. Cell. 2002; 109(1):75–86. [PubMed: 11955448]

Maciejczyk P, et al. Effects of subchronic exposures to concentrated ambient particles (CAPs) in mice. II. The design of a CAPs exposure system for biometric telemetry monitoring. Inhal. Toxicol. 2005; 17(4–5):189–197. [PubMed: 15804936]

Mack CM, et al. Sex-Differences in the Distribution of Axon Types within the Genu of the Rat Corpus-Callosum. Brain Res. 1995; 697(1–2):152–156. [PubMed: 8593571]

Mathew P, et al. Maturation of corpus callosum anterior midbody is associated with neonatal motor function in eight preterm-born infants. Neural Plast. 2013; 2013:359532. [PubMed: 23509639]

McPhillips M, et al. Motor deficits in children with autism spectrum disorder: a cross-syndrome study. Autism Res. 2014; 7(6):664–676. [PubMed: 25258309]

Mehlhase J, et al. Ferritin levels in microglia depend upon activation: modulation by reactive oxygen species. Biochim. Biophys. Acta. 2006; 1763(8):854–859. [PubMed: 16777245]

Mei F, et al. Stage-specific deletion of Olig2 conveys opposing functions on differentiation and maturation of oligodendrocytes. J. Neurosci. 2013; 33(19):8454–8462. [PubMed: 23658182]

Rowitch DH. Glial specification in the vertebrate neural tube. Nat. Rev. Neurosci. 2004; 5(5):409–419. [PubMed: 15100723]

Rowitch DH, Kriegstein AR. Developmental genetics of vertebrate glial-cell specification. Nature. 2010; 468(7321):214–222. [PubMed: 21068830]

Schulte T, Muller-Oehring EM. Contribution of callosal connections to the interhemispheric integration of visuomotor and cognitive processes. Neuropsychol. Rev. 2010; 20(2):174–190. [PubMed: 20411431]

Sun YL, et al. The air-borne particulate pollution in Beijing - concentration, composition, distribution and sources. Atmos. Environ. 2004; 38(35):5991–6004.

Takebayashi H, et al. The basic helix-loop-helix factor Olig2 is essential for the development of motoneuron and oligodendrocyte lineages. Curr. Biol. 2002; 12(13):1157–1163. [PubMed: 12121626]

Talbott EO, et al. Fine particulate matter and the risk of autism spectrum disorder. Environ. Res. 2015; 140:414–420. [PubMed: 25957837]

Tanaka-Arakawa MM, et al. Developmental changes in the corpus callosum from infancy to early adulthood: a structural magnetic resonance imaging study. PLoS One. 2015; 10(3):e0118760. [PubMed: 25790124]

Traiffort E, et al. Hedgehog: A Key Signaling in the Development of the Oligodendrocyte Lineage. J Dev Biol. 2016; 4(3):28–28.

Travers BG, et al. Atypical development of white matter microstructure of the corpus callosum in males with autism: a longitudinal investigation. Mol. Autism. 2015; 6(1):15. [PubMed: 25774283]

Vincze A, et al. A correlative light and electron microscopic study of postnatal myelination in the murine corpus callosum. Int. J. Dev. Neurosci. 2008; 26(6):575–584. [PubMed: 18556167]

Vojinovic S, et al. Disease relapses in multiple sclerosis can be influenced by air pollution and climate seasonal conditions. Vojnosanit. Pregl. 2015; 72(1):44–49. [PubMed: 26043590]

Volk HE, et al. Traffic-related air pollution, particulate matter, and autism. JAMA Psychiatry. 2013; 70(1):71–77. [PubMed: 23404082]

Volpe JJ, et al. The developing oligodendrocyte: key cellular target in brain injury in the premature infant. Int. J. Dev. Neurosci. 2011; 29(4):423–440. [PubMed: 21382469]

Wang J, et al. Transcription factor induction of human oligodendrocyte progenitor fate and differentiation. Proc. Natl. Acad. Sci. U. S. A. 2014; 111(28):E2885–2894. [PubMed: 24982138]

Wang Y, et al. Microglial activation, recruitment and phagocytosis as linked phenomena in ferric oxide nanoparticle exposure. Toxicol. Lett. 2011; 205(1):26–37. [PubMed: 21596115]

Wolff JJ, et al. Differences in white matter fiber tract development present from 6 to 24 months in infants with autism. Am. J. Psychiatry. 2012; 169(6):589–600. [PubMed: 22362397]

Zhou Q, Anderson DJ. The bHLH transcription factors OLIG2 and OLIG1 couple neuronal and glial subtype specification. Cell. 2002; 109(1):61–73. [PubMed: 11955447]

Zhu X, et al. Olig2-dependent developmental fate switch of NG2 cells. Development. 2012; 139(13): 2299–2307. [PubMed: 22627280]

Highlights

- Exposure to particulate matter (PM) during fetal development is neurotoxic.
- Gestational PM exposure accelerates oligodendrocyte precursor maturation.
- Gestational PM exposure induces persistent corpus callosum (CC) hypermyelination.
- Gestational PM exposure persistently alters the CC oligodendrocyte progenitor pool.

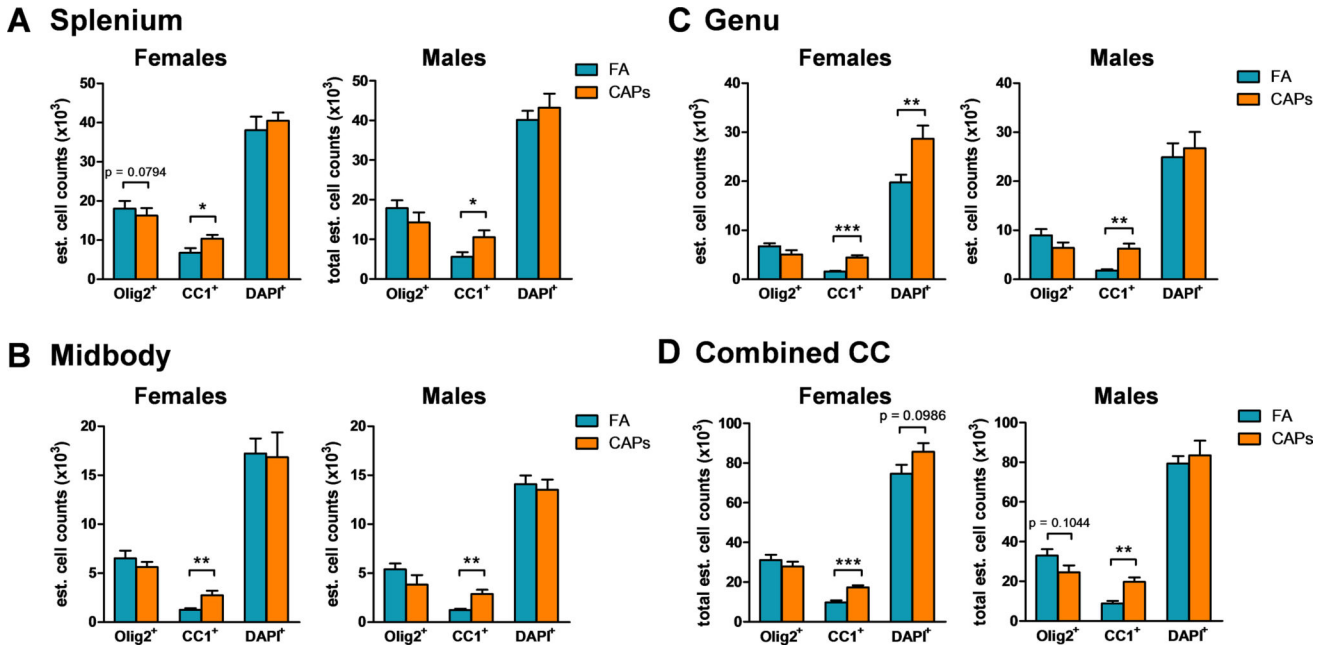

Figure 1. Gestational exposure to CAPs decreases the number of immature oligodendrocytes and increases the number of mature oligodendrocytes in the CC at PND11–15

Tissue was immunofluorescently labeled for Olig2, CC-1, and DAPI. **A)** CAPs significantly increases CC-1$^+$ cells in the caudal splenium sub-region of the CC in males and females, and decreases Olig2$^+$ cells in the female splenium. **B)** In the central midbody sub-region of the CC, CAPs exposure significantly increases the number of CC-1$^+$ cells in males and females. **C)** CC-1$^+$ numbers were significantly increased in the male and female genu, the most rostral subregion of the CC, with a co-occurring significant increase in DAPI$^+$ cells in the female genu. **D)** Total estimates of positive staining in the CC indicates an overall increase in CC-1$^+$ cells across both sexes with a trending decrease in Olig2$^+$ cells in the male CC. Data represent mean ± SEM of estimates across 3 serial tissue sections analyzed by one-way ANOVA (N = 6–11/group). *$p < 0.05$, **$p < 0.01$, ***$p < 0.0001$.

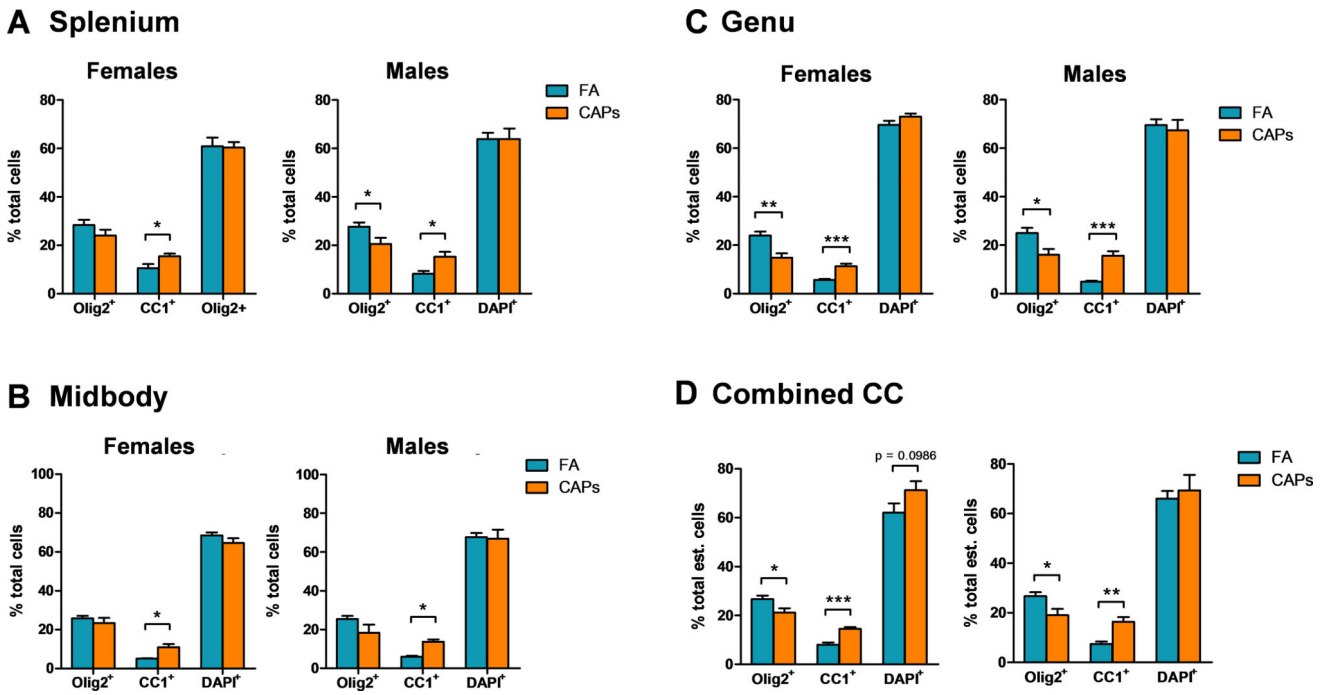

Figure 2. CAPs exposure proportionally shifts CC oligodendrocytes towards a more mature phenotype at PND11–15

Stereological cell counts are expressed as a percent of total counted cells by CC sub-region and total CC. **A)** The proportion of mature CC-1$^+$ oligodendrocytes is significantly increased in the splenium of males and females. In the male splenium, CAPs exposure significantly decreased the proportion of Olig2$^+$ cells. **B)** In the midbody, only the proportion of CC-1$^+$ cells was significantly increased by CAPs exposure in both sexes. **C)** Both the male and female genu experience a significant proportional decrease in Olig2 staining and a significant increase in CC-1 staining. **D)** Across the entire CC, there is a significant decrease in Olig2 staining with a corresponding increase in CC-1 staining. Additionally, there is a trending increase in the proportion of DAPI$^+$ cells across the CC of CAPs-treated females. Data represent mean ± SEM of estimates across 3 serial tissue sections analyzed by one-way ANOVA (N = 6–11/group). *$p < 0.05$, **$p < 0.01$, ***$p < 0.0001$.

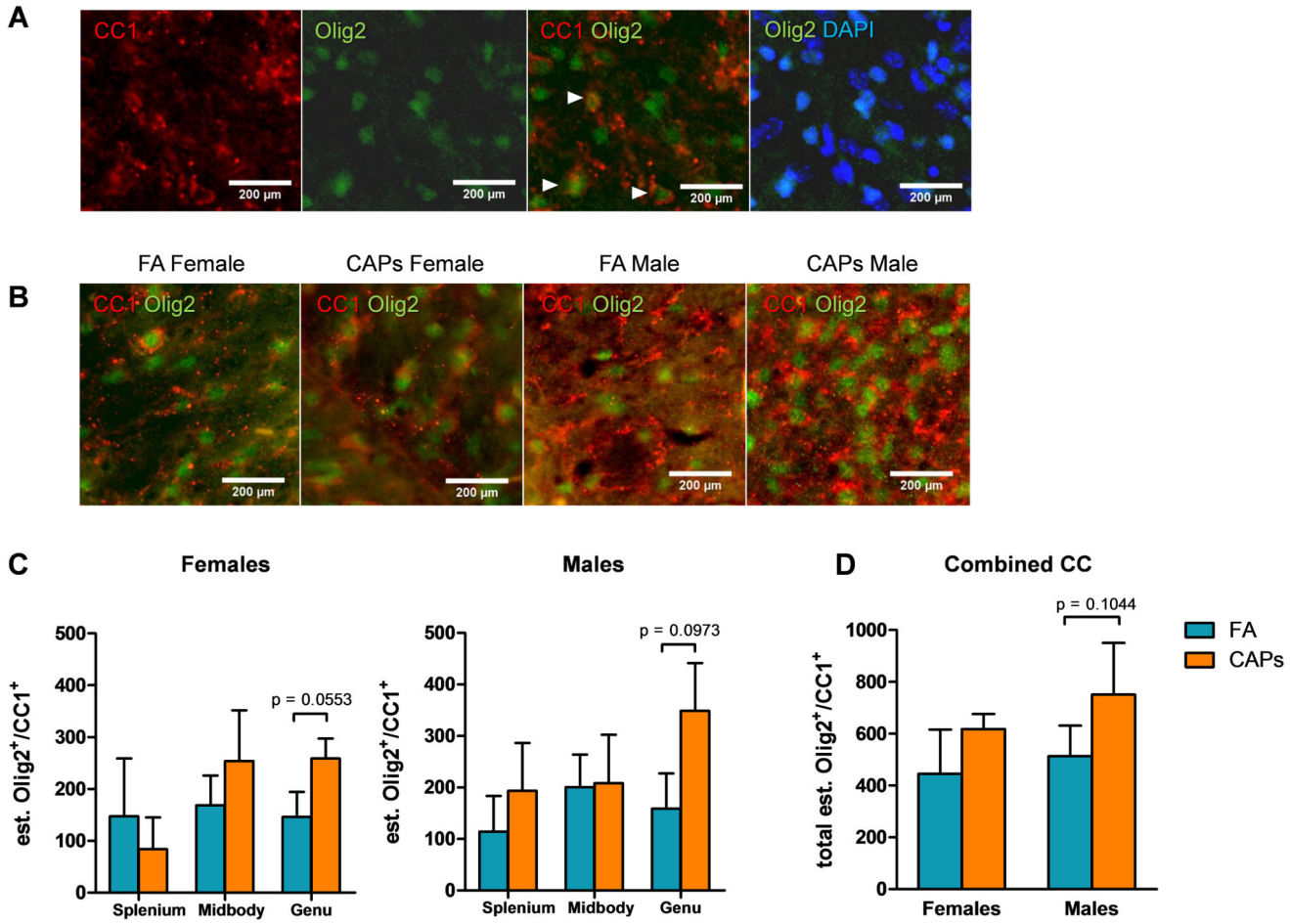

Figure 3. CAPs exposure increases Olig2$^+$/CC-1$^+$ cells across the CC and CC sub-regions at PND11–15

Gestational exposure to CAPs significantly elevated the number of mature Olig2$^+$/CC-1$^+$ double-positive cells in the genu of the CC during the postnatal period (PNDs 11–15). **A)** Representative micrographs of CC-1, Olig2, Olig2/CC-1 merge, and Olig2/DAPI merge from the splenium of a control male to demonstrate each of the staining patterns. Arrows indicate locations of Olig2$^+$/CC-1$^+$ cells where staining co-localizes in the z-plane. **B)** Representative micrographs of Olig2$^+$/CC-1$^+$ staining in the genu, where Olig2$^+$/CC-1$^+$ numbers were significantly elevated (quantified in **C**). Images were taken at 40× magnification. Data represent mean ± SEM of estimates across 3 serial tissue sections analyzed by one-way ANOVA. *$p < 0.05$, **p < 0.01, ***$p < 0.0001$.

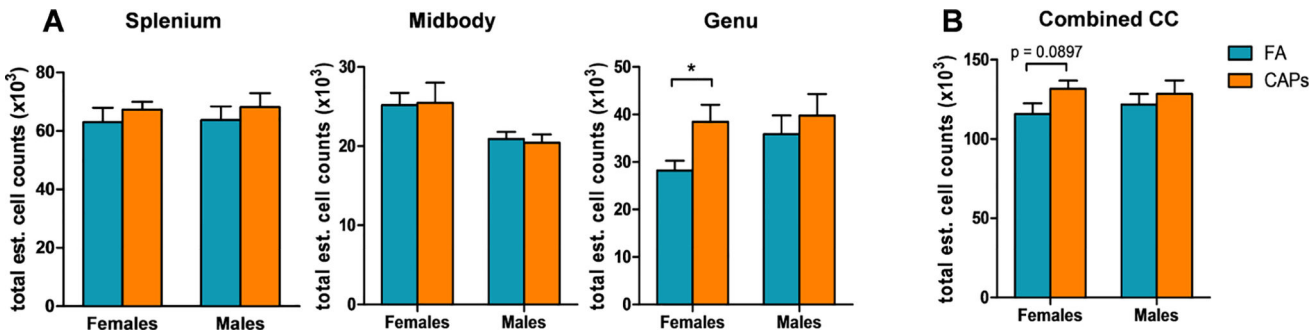

Figure 4. The female genu experiences elevation in cell number as a result of CAPs exposure during gestation, but total CC cellularity as a whole is not affected at PND11–15

A) Total cell numbers across the CC were generated from Olig2/CC-1/DAPI stereological analyses. The splenium and midbody sub-regional cellularity were unaffected by gestational CAPs exposure, however, the female genu was significantly affected by CAPs exposure and had significant cell number elevation in this sub-region. **B)** When considering the CC structure as a whole, gestational CAPs exposure did not significantly alter cell number in the CC. Data represent mean ± SEM of estimates across 3 serial tissue sections analyzed by one-way ANOVA (N = 6–11/group). *$p < 0.05$.

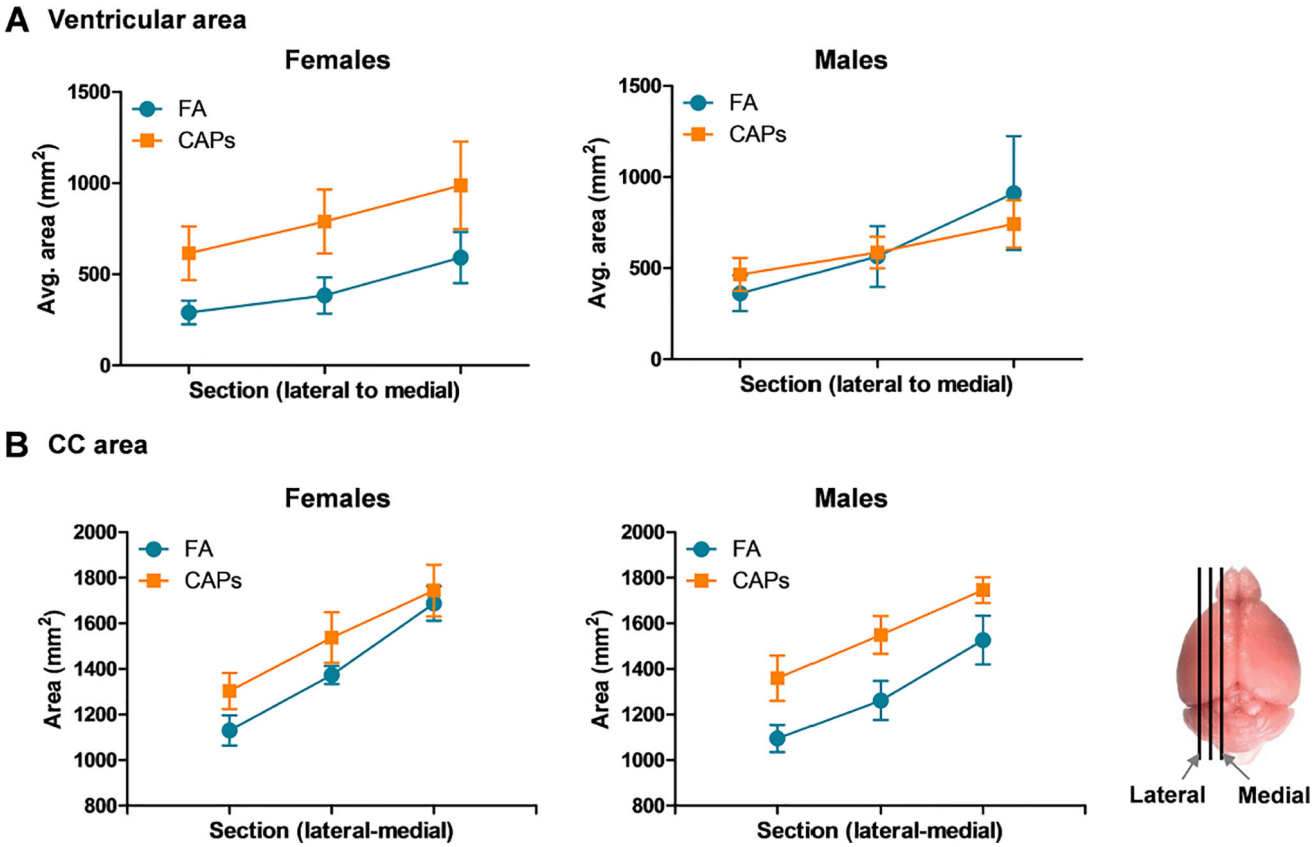

Figure 5. Gestational CAPs exposure results in persistent ventriculomegaly and elevated CC area in a sex-specific manner at PND57–61

The area of the lateral ventricles and CC were traced using Neurolucida and graphed such that each data point represents a single tissue section, from the lateral-most section to the medial-most section (approximate sampled areas indicated to right of panel **B**). **A)** Lateral ventricle area is persistently elevated at PNDs 57–61 in CAPs-exposed females ($p = 0.08$), but there is no persistent effect of CAPs exposure in males. **B)** Gestational CAPs exposure persistently elevates CC area in both males and females. Statistical outcome for CC area: main effect of CAPs across sexes ($p = 0.013$) and a CAPs by PND interaction ($p = 0.019$). Data represent mean ± SEM of 3 serial sections of brain tissue (N = 7–9/group).

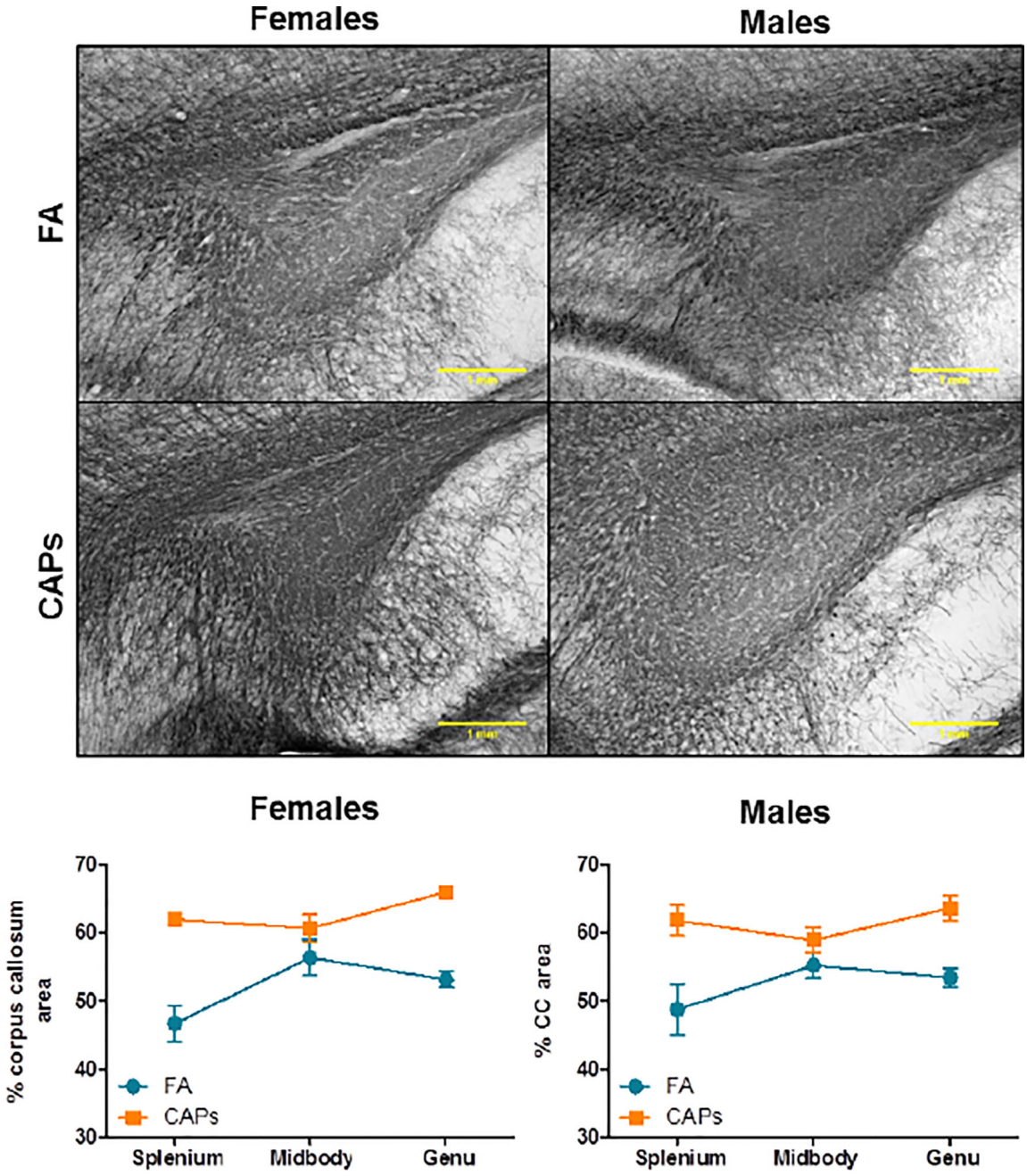

Figure 6. CAPs exposure induces persistently increases in myelin basic protein expression in the CC at PND57–61

CAPs significantly increased MBP density across the three major regions indicated: genu (rostral portion), midbody (central portion), and splenium (caudal portion) in the mature brain (PNDs 57–61). Scale bars represent 1mm distance. **A)** Representative micrographs of PND15 splenium at 10× magnification. **B)** Data is expressed as a percent of CC area positively stained for MBP. Statistical outcome: main effect of CAPs across sexes ($p < 0.0001$). Data represent mean ± SEM of 3 serial sections of brain tissue (N = 7–9/group).

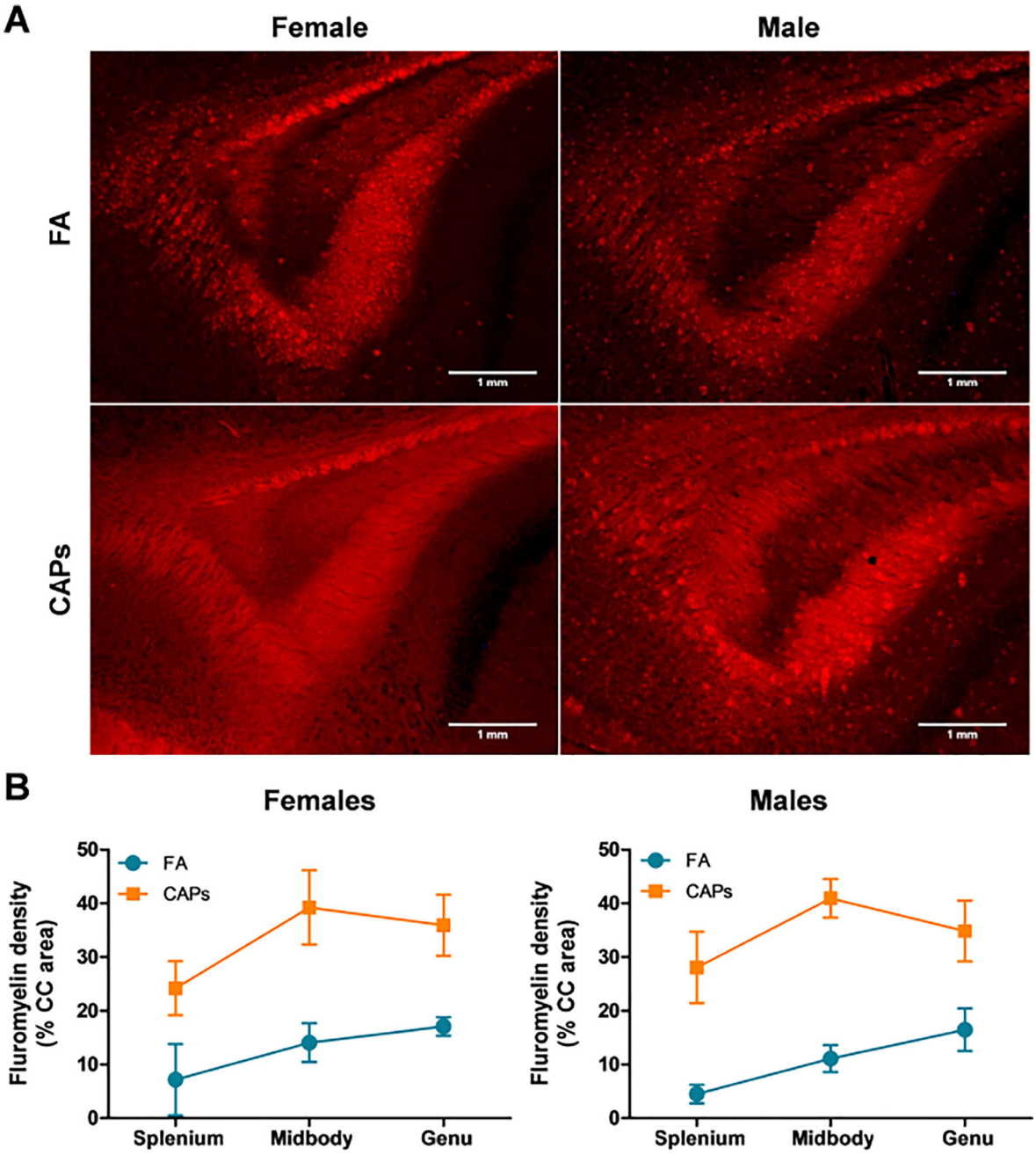

Figure 7. Gestational CAPs exposure persistently elevates compact myelin density in the CC at PND57–61

CAPs significantly increased compact myelin, as indicated by FluoroMyelin Red staining density, across the three major regions indicated: genu (rostral portion), midbody (central portion), and splenium (caudal portion). **A)** Representative micrographs of PND61 splenium at 10× magnification. Scale bars represent 1mm distance. **B)** Data is expressed as a percent of CC area positively stained by FluoroMyelin. Statistical outcome: main effect of CAPs across sexes ($p < 0.0001$); main effect of PND ($p = 0.0022$). Data represent mean ± SEM of 3 serial sections of brain tissue (N = 7–9/group).

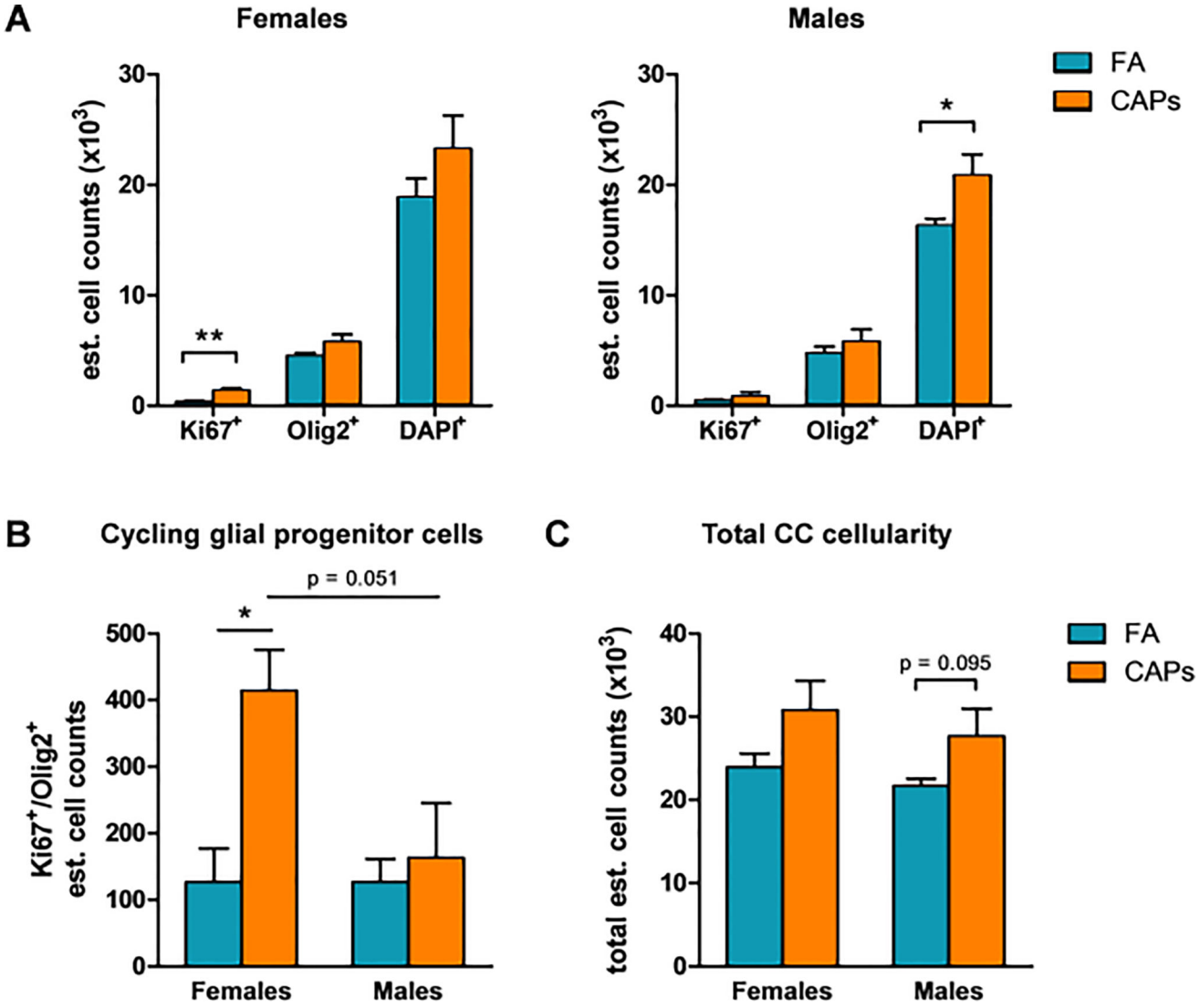

Figure 8. Gestational CAPs exposure persistently alters the cellularity and proliferative capacity of OPCs in the CC at PND57–61

Tissue of exposed animals was harvested at PNDs 57–61 and analyzed for Ki67 and Olig2 fluorescent immunoreactivity with a DAPI nuclear stain. **A)** CAPs exposure significantly elevated the estimated number of singly-stained $Ki67^+$ cells in the female CC and the number of $DAPI^+$ cells in the male CC. There was no significant effect of CAPs exposure on the numnber of $Olig2^+$ cells. **B)** CAPs exposure significantly increased the number of double-positive $Ki67^+/Olig2^+$ OPCs in the female CC. There was a marginally significant effect of sex among CAPs-exposed animals ($p = 0.051$). **C)** CAPs exposure elevates the total number of cells in the CC, though this effect is not significant. Data represent mean ± SEM of estimates across 3 serial tissue sections analyzed by one-way ANOVA (N = 4–5/group). $*p < 0.05$, $**p < 0.01$.

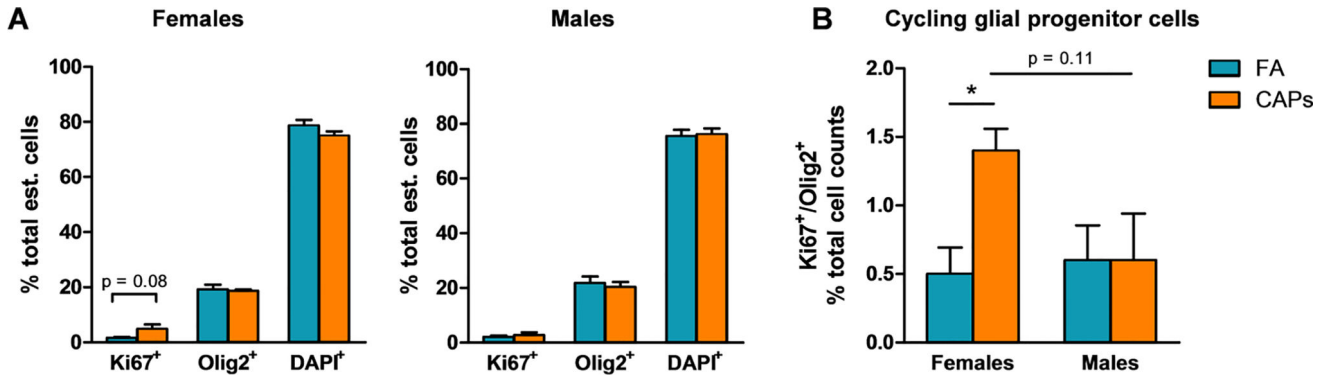

Figure 9. Gestational CAPs exposure persistently elevates the proportion of proliferative OPCs in the female CC at PND57–61

Tissue of exposed animals was harvested at PNDs 57–61 and analyzed for Ki67 and Olig2 fluorescent immunoreactivity with a DAPI nuclear stain. **A)** The proportion of singly-stained $Ki67^+$ cells in the female CC was elevated with trending significance ($p = 0.08$) with no effect on $Olig2^+$ or $DAPI^+$ cells as a result of CAPs exposure. There was no effect of CAPs on the proportion of singly-stained $Ki67^+$, $Olig2^+$, or $DAPI^+$ cells in the male CC. **B)** Gestational CAPs exposure significant elevates the proportion of double-positive $Ki67^+$/$Olig2^+$ cells in the female CC but not in the male CC. There was a trending effect of sex among CAPs-exposed animals ($p = 0.11$). Data represent mean ± SEM of estimates across 3 serial tissue sections analyzed by one-way ANOVA (N = 4–5/group). *$p < 0.05$.